

CLOSE RANGE PHOTOGRAMMETRY USED FOR THE MONITORING OF HARBOUR BREAKWATERS

M. Hennau^{a,*}, A. De Wulf^b, R. Goossens^a, D. Van Damme^a, J. De Rouck^b, P. Hanssens^c, L. Van Damme^d

^a Department of Geography, Ghent University, Krijgslaan 281 S8, 9000 Ghent, Belgium - Marc.Hennau@ugent.be

^b Department of Coastal Engineering, Ghent University, Technologiepark Zwijnaarde 904, 9052 Zwijnaarde, Belgium - Julien.DeRouck@ugent.be

^c VLG-LIN-AWZ-Waterwegen Kust, Rederskaai 50, 8380 Zeebrugge, Belgium - Paul.Hanssens@lin.vlaanderen.be

^d VO-MOW-Maritieme Toegang-Cel Kusthavens, Vrijhavenstraat 3, 8400 Oostende, Belgium - Luc.Vandamme@lin.vlaanderen.be

KEY WORDS: Digital, Reconstruction, Close Range, Photogrammetry, Measurement, Method

ABSTRACT:

Breakwaters are constructed to protect harbours against the destructive power of the sea. The top layer of rubble mound breakwaters is often composed of clear-cut concrete armour units. With the aim to maintain the integrity of these breakwaters, the units have to stay within their original pattern. Therefore, breakwaters have to be accurately monitored in order to detect any shift in position of any of the concrete armour units. A specific methodology, combining surveying and close range photogrammetric techniques, has been developed by Ghent University to perform the monitoring of the concrete armour units on breakwaters and was tested at the seaport of Zeebrugge.

1. INTRODUCTION

Worldwide, breakwaters are erected to shield outer seaport facilities from the destructive power of waves. In 1976, a rubble mound type of breakwater was selected for the protection of the expanding outer port of Zeebrugge (Fig.1).

The main constructions, which required state of the art civil engineering methods, were finished in 1985. The top layer of the breakwaters is composed of clear-cut concrete armour units which were specially positioned in order to dissipate the wave energy (Fig.2).

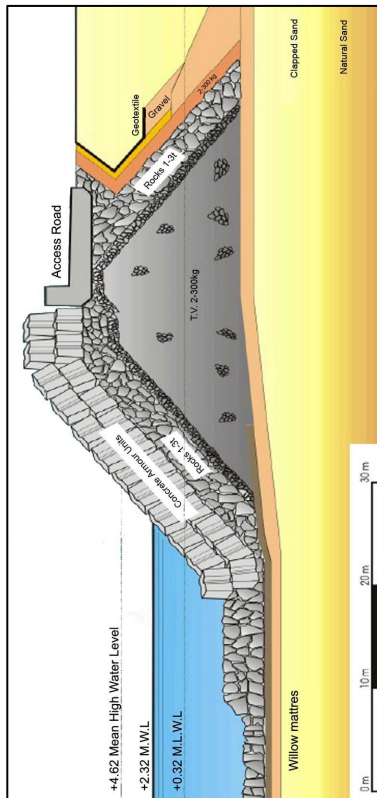


Figure 1. Cross section of the breakwater at Zeebrugge

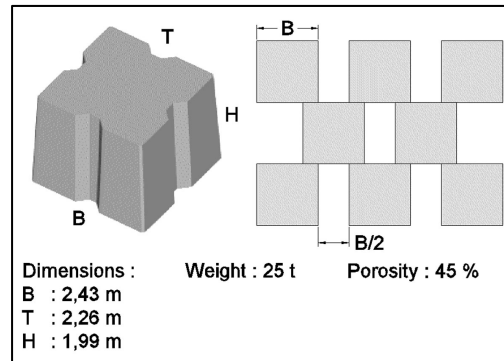


Figure 2. Concrete armour unit and front view of the original placement pattern

Unfortunately, subsidence of the different layers is unavoidable over the years. With the aim to maintain the integrity and function of the breakwaters, the pattern changes in the cover layer have to stay within acceptable boundaries and therefore the concrete armour units must be carefully monitored.

A specific methodology, combining surveying and close range photogrammetric techniques, has been developed by Ghent University to perform the monitoring of concrete armour units and was tested at the seaport of Zeebrugge, on a 500m long part of the western breakwater. During development, special attention was given to the optimization of the geometrical accuracy of the different steps. This paper will discuss the separate semi-automated processes of the developed methodology in chronological order.

* Corresponding author

2. METHODOLOGY

2.1 Survey

2.1.1 Topography: First of all, a new reference network, consisting of a chain of topographic nails, had to be materialized on the breakwater and related to the Belgian Lambert '72 planimetric coordinate system (BD72) and altimetric TAW level. A series of photogrammetric beacons, with centred topographic nails, was subsequently added to the reference network along the test site. The planimetric positions of the new reference points and the centres of the photogrammetric beacons together with the existing harbour reference poles were measured using the topographic forced centring surveying technique. Angle and distance measurements were carried out with a Leica TC1610 total station (1,5" angle accuracy and 2mm + 2ppm distance measurement accuracy, according to DIN 18723). Both reference points and photogrammetric beacons were leveled using a Zeiss DIN11T (nominal accuracy 0,3mm/km) in combination with an invar rod. Based upon the known coordinates of the harbour reference poles, the new reference network was transformed into the Belgian coordinate system.

2.1.2 Photography: The second part of the fieldwork consisted of close range photogrammetric shots along the test site. A series of high-resolution digital photos covering the breakwater was taken from a telescopic mobile crane (SK598-AT5) with a Canon EOS-1ds fitted with a lens with a calibrated focal length of 24,513 mm. The photos were taken nearly vertically with theoretic interval distances of 25m and overlaps of 60% in order to form a photogrammetric strip with its simulated flight line centred above the top of the mound and parallel to the breakwater on an altitude of ca. 50m above the access road (Fig.3).

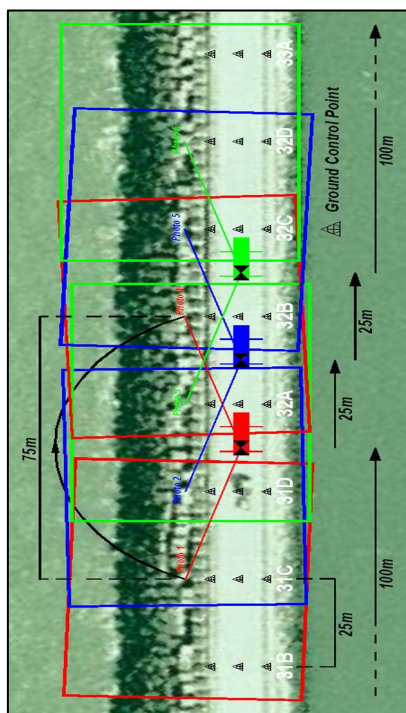


Figure 3. Photogrammetric strip

Given these parameters, a photo scale of 1:1800 and shot angles of 74 by 53 degrees were achieved. Simultaneously, approximate coordinates for the centre of projection of the camera were measured by a differential code satellite positioning system (Leica SR-20 series). The photogrammetric beacons were materialized every 25m crosswise on the access road and central wall in order to provide the overlapping photo couples with at least six common ground control points.

2.2 Digital processing

2.2.1 Photogrammetry: Digital photogrammetric processing was carried out on the photogrammetric workstation Strabox* in combination with the GIS software Orbit* and its photogrammetric extension Strabo*.

Photo coordinates were measured for the ground control points, but as the beacons were all located on the upper half of the photos, photo coordinates of extra tie points were measured on the concrete armour units of the breakwater, which were situated on the lower part of the photos. Combining the approximate BD72 coordinates of the centres of projection and the BD72 coordinates of the ground control points with the photo coordinates of both ground control points and tie points, the photo strip was digitally oriented using aerotriangulation techniques and bundle block adjustment. Consequently, the breakwater was projected into the Strabox in stereo vision, which made it possible to manually measure 3D coordinates in the stereo models.

The almost cubic shaped concrete armour units were produced with clear-cut dimensions. Because of the harsh physical conditions on the breakwater, the concrete armour units are heavily weathered. Therefore, the exact vertices of the units were almost impossible to identify, excluding a straightforward measurement of a unit's position. To overcome this problem, a stepwise method was implemented to determine the positions of the units. Firstly, the most visible side of each unit, which was the top side in 99%, was considered. Secondly, two points were measured on each of the four main edges of the selected side (Fig. 4), yielding redundant geometric information, which was used for control purposes.

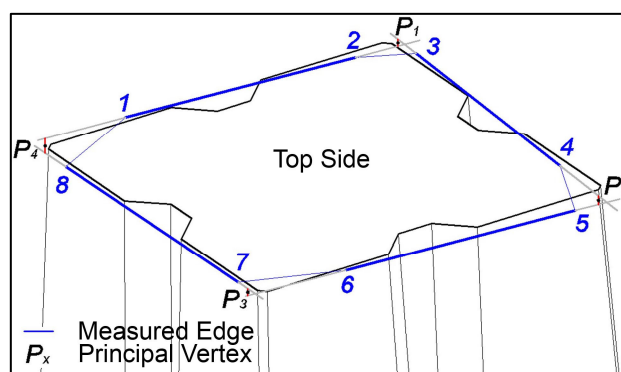


Figure 4. Top side determined by 8 points

It wasn't possible to measure eight points for every unit due to stereo occlusion. 14% of the units were determined by an alternate amount of points, ranging from seven to a minimum of three points.

* TM Eurotronics NV. Belgium

2.2.2 Automated coordinate computation: In case of eight measured points, the spatial equations of the non-intersecting edge fractions were used to compute the coordinates of four principal vertices of the considered side. In doing so, the shape of the unit's side was generalised to a square in case of a top side and to a trapezium in case of a flank side, although it must be said that the four principal vertices were non-coplanar after computation.

To compute the coordinates of one principal vertex (P₁), the common perpendicular straight line to the involved edge fractions was firstly determined (Fig. 5).

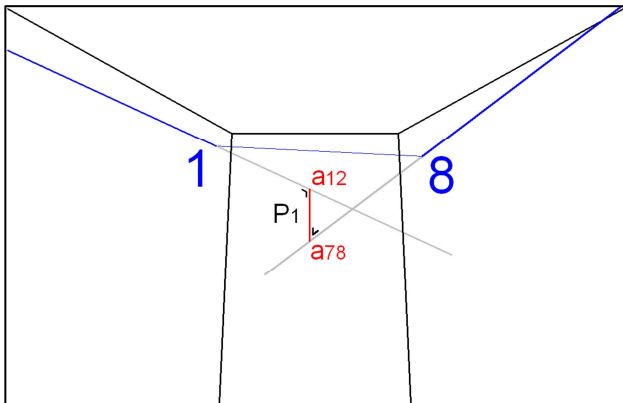


Figure 5. Constructed common perpendicular straight line

As stated in the following equation, the length of the two involved edge fractions and the distances from the points of intersection, between common the perpendicular straight line and the edge lines, to the adjacent points of the respective edge fractions were taken into account in the determination of the principal vertex.

$$P_1 = \frac{(a_{12} \times [1,2]) + (a_{78} \times [7,8])}{[1,2] + [7,8]} + \frac{(a_{12} \times [8, a_{78}]) + (a_{78} \times [1, a_{12}])}{[1, a_{12}] + [8, a_{78}]}$$

where p_1 = coordinates principal vertex
 1,2,7,8 = measured edge points
 a_{12}, a_{78} = coordinates points of intersection
 [a,b] = length straight fractions

For the edges determined by less than 2 points, some basic rules were established concerning the computation of the spatial equation of these edges and for the subsequent computation of the 2 principal vertices related to these edges. Finally, a side with theoretical dimensions was fitted on the four non-coplanar principal vertices, using a three dimensional conformal transformation.

2.2.3 Reconstructing the top layer of the breakwater, a theoretic volume model of the armour unit was fit to each computed side (Fig.6).

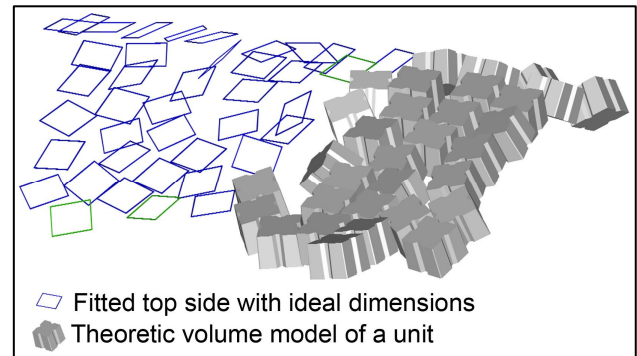


Figure 6. Reconstructed top layer

To check the accuracy of the process, a second reconstruction of a portion of the test site was performed based on an independent photogrammetric strip.

3. TEST RESULTS

3.1 Topography

After least square adjustment, the topographic survey resulted in a mean standard deviation of 9mm in planimetry for both reference points and photogrammetric beacons. The independent levelling of all new materialized points resulted in a mean standard deviation of 2mm in altimetry.

3.2 Photogrammetry

Mean standard deviations were computed for ground control points and tie points after the bundle block adjustments of the complete test strip (Table 7) and the control strip (Table 8).

Mean Standard Deviation GCPs (m)		
X	Y	Z
0,013	0,014	0,033
Mean Standard Deviation TPs (m)		
X	Y	Z
0,028	0,027	0,079

Table 7. Results bundle block adjustment test strip

Mean Standard Deviation GCPs (m)		
X	Y	Z
0,012	0,011	0,031
Mean Standard Deviation TPs (m)		
X	Y	Z
0,024	0,025	0,075

Table 8. Results bundle block adjustment control strip

3.3 Reconstruction breakwater

Residues and standard deviation for the coordinates of the four fitted principal vertices were calculated during the three dimensional conformal transformation of an ideal unit side upon each set of computed principal vertices. Coordinates of the centre of the fitted ideal side were also computed, marking each unit with a single point.

A first classification of measured units was made based on the type of measured side and on the number of measured points per side (Table 9). The altimetric position of the centre points was the basis for a second classification (Table 10). Mean standard deviations after transformation were used as comparison criteria between unit classes.

Mean Standard Deviation after Transformation (m)							
Side	#pts	#units	%	mXYZ	mX	mY	mZ
All		1301	100,0	0,096	0,041	0,037	0,074
Top	8	1118	85,9	0,094	0,040	0,035	0,074
	7	55	4,2	0,112	0,050	0,045	0,084
	6	70	5,4	0,112	0,047	0,050	0,082
	4	44	3,4	0,080	0,042	0,042	0,052
Flank	8	6	0,5	0,100	0,057	0,054	0,057
	7	1	0,1	0,081	0,042	0,039	0,057
	6	4	0,3	0,180	0,114	0,085	0,106
	4	3	0,2	0,141	0,078	0,099	0,056

Table 9.

One can notice that the relative planimetric accuracy of the measurements within the stereo models is two times better than the altimetric accuracy.

Mean Standard Deviation within Altimetric Class (m)						
Level	#units	%	mXYZ	mX	mY	mZ
0-2m	97	7,5	0,119	0,056	0,052	0,086
2-4m	204	15,7	0,126	0,055	0,050	0,096
4-6m	219	16,8	0,109	0,047	0,040	0,085
6-8m	204	15,7	0,096	0,043	0,036	0,073
8-10m	235	18,1	0,083	0,036	0,030	0,064
10-12m	342	26,3	0,072	0,027	0,028	0,057

Table 10.

Measurement accuracies are clearly lower for units at the base of the breakwater as shown in table 10.

Standard deviations after transformation are also strongly correlated to the altimetric position of the units on the breakwater as illustrated on diagram 11.

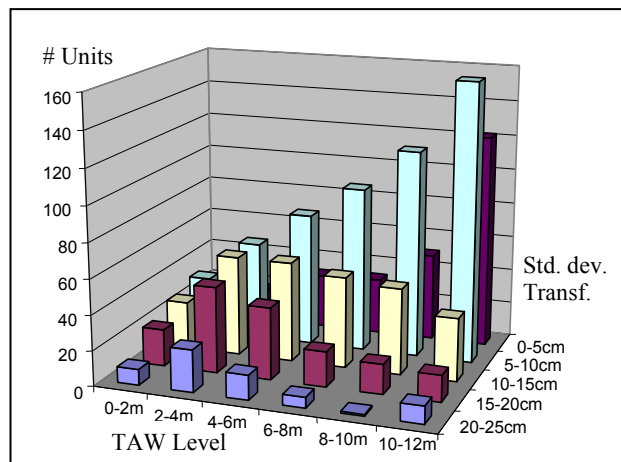


Diagram 11. Correlation between altimetric position and measurement accuracy

The results of the transformation of the independent control units and their original counterparts are fairly comparable, as shown in tables 12 and 13.

Mean Standard Deviation (m)							
Control Strip							
Side	#pts	#units	%	mXYZ	mX	mY	mZ
All		224	100,0	0,089	0,043	0,033	0,065
Top	8	203	90,6	0,090	0,042	0,033	0,067
	7	12	5,4	0,090	0,050	0,036	0,055
	6	3	1,3	0,090	0,040	0,057	0,052
	4	6	2,7	0,055	0,034	0,028	0,033

Table 12. Results control strip

Mean Standard Deviation (m)							
Original Strip							
Side	#pts	#units	%	mXYZ	mX	mY	mZ
All		224	100,0	0,097	0,044	0,037	0,074
Top	8	203	90,6	0,098	0,043	0,037	0,074
	7	12	5,4	0,086	0,047	0,038	0,060
	6	3	1,3	0,094	0,039	0,041	0,072
	4	6	2,7	0,099	0,058	0,045	0,065

Table 13. Results counterparts original strip

The control of the process was based on the computation of differences between the coordinates of the side centres of 224 units and their control counterparts (Table 14).

Mean Differences (m)				
All units				
	X	Y	Z	XYZ
	0,016	0,016	0,054	0,063
Classified according to altimetric level				
Level	X	Y	Z	XYZ
0-2m	0,082	0,062	0,077	0,139
2-4m	0,018	0,029	0,069	0,080
4-6m	0,023	0,019	0,060	0,072
6-8m	0,013	0,016	0,068	0,075
8-10m	0,012	0,008	0,041	0,046
10-12m	0,013	0,011	0,044	0,050

Table 14. Differences between original and control strip

4. CONCLUSIONS

Photo scale differences between the units on the top of the mound and at the base of the breakwater, the important height difference (+8m), in view of the photo scale, between the ground control points and the base units and the presence of seaweed at the base of the breakwater, makes the measurement of base layered units within the stereo models more difficult and less precise. Bigger standard deviations after bundle block adjustment for the tie points, measured at the base of the breakwater, and the apparent lower relative measurement accuracy in the stereo models for the lower altimetric unit classes (Table 10), support these findings.

Given the results of the control measurement, relative measurement accuracies, reflected by the standard deviation computed after fitting of an ideal unit to a measured unit, can be replicated by the applied processes. Furthermore, mean differences between original measurements and control measurements (Table 14) are well within the computed relative measurement accuracies as shown in table 9.

Given the results of the comparison between the measurements on the original strip and the control strip, it can be stated that the developed methodology can be replicated.

